Available online at www.sciencedirect.com
ScienceDirect
Ceramics International 38 (2012) 649–655
CERAMICS INTERNATIONAL
www.elsevier.com/locate/ceramint

Microstructure and mechanical properties of in situ synthesized (TiB2 + TiC)/Ti3SiC2 composites

Jian Yang *, Limei Pan, Wei Gu, Tai Qiu, Yuzhe Zhang, Shemin Zhu

College of Materials Science and Engineering, Nanjing University of Technology, Nanjing 210009, China

Received 30 August 2010; received in revised form 4 April 2011; accepted 28 June 2011
Available online 30th July 2011

Abstract

Based on thermodynamic analysis, highly dense (TiB_2 + TiC)/Ti_3SiC_2 composite ceramics with different TiB_2 volume contents were in situ fabricated in situ by hot-pressing at 1500 °C. Laminar Ti_3SiC_2 grains, columnar TiB_2 grains and equiaxed TiC grains were clearly identified from microstructural observation; grain boundaries were clean. The increase of TiB_2 volume content significantly restrains the grain growth of the Ti_3SiC_2 matrix. As the content of TiB_2 increases from 5 vol.% to 20 vol.%, the bending strength and fracture toughness of the composites both increase and then decrease, whereas the Vickers hardness increases linearly from 6.13 GPa to 11.5 GPa. The composite with 10 vol.% TiB_2 shows the optimized microstructure and optimal mechanical properties: 700 MPa for bending strength; 9.55 MPa $m^{1/2}$ for fracture toughness. These are attributed to the synergistic action of strengthening and toughening mechanisms such as particulate reinforcement, crack deflection, grain's pull-out and fine-grain toughening, caused by the columnar TiB_2 grains and equiaxed TiC grains.

Keywords: C. Mechanical properties; (TiB_2 + TiC)/Ti_3SiC_2 composites; In situ synthesis; Microstructure

1. Introduction

Ti_3SiC_2 is a ternary layered carbide. It is considered a potential structural/functional material for its combined metallic- and ceramic-like properties, such as low density, high modulus, good thermal and electrical conductivity, excellent thermal shock resistance and high temperature strength, damage tolerance and easy machinability [1–5]. However, its low hardness and low creep strength restrict the potential application of Ti_3SiC_2 as a high-temperature structural material. Incorporation of second phase is an effective way to overcome these weaknesses. A number of reinforcing agents including TiC, SiC, Al_2O_3, c-BN, TiB_2 and ZrO_2 have been applied to improve the mechanical properties of Ti_3SiC_2 [6–11]. However, previous studies concentrated on composites containing only one reinforcing agent which showed a limited enhancement effect. In recent years, a synergy mechanism between two or more strengthening and toughening methods was reported. By this mechanism, the enhancement and toughening effect was usually larger than the additional effect brought by individual toughening mechanisms. Chen et al. [12] prepared (TiC + Al_2O_3)/Ti_3AlC_2 composite ceramics by a combustion reaction, which show higher flexural strength and Vickers hardness than pure Ti_3AlC_2 ceramic. Zan et al. [13] added the SiC whiskers as 2nd-level toughening agent into Al_2O_3 layers in Al_2O_3/Ti_3SiC_2 multilayer ceramics. Excellent bending strength (688 MPa) and work of fracture (2583 J/m^2) were obtained due to combined 1st-level toughening mechanism (multilayer structural toughening) and 2nd-level toughening mechanism (whisker toughening). Various other well-known strengthening and toughening mechanisms can also be used for the design of ceramics.

Owing to the promising properties such as high hardness, high modulus, excellent chemical stability, good electrical and thermal conductivity, and similar coefficient of thermal expansion (CTE) to Ti_3SiC_2, both TiB_2 and TiC are ideal candidate reinforcements for Ti_3SiC_2 matrix [7,10]. As reinforcing agents, TiC grains usually are equiaxed and provide dispersion strengthening effect, whereas TiB_2, produced by in situ reaction process, usually is columnar/plate like grain, which can play a role similar to whisker toughening [14].

* Corresponding author. Tel.: +86 25 83587262; fax: +86 25 83587268.
E-mail address: yangjian1976@163.com (J. Yang).

0272-8842/$36.00
doi:10.1016/j.ceramint.2011.06.066

Comparing to traditional preparation process, in situ synthesis shows many advantages in fabrication of composite ceramics, such as uniform distribution and fine grain size of reinforcements, clean and tightly bonded grain boundary, simplified process and excellent properties [15]. Therefore, in the present investigation, (TiB_2 + TiC)/Ti_3SiC_2 composites were prepared by in situ hot-pressing sintering, in which Ti_3SiC_2 matrix was synergistically reinforced by columnar TiB_2 and equiaxed TiC grains. Effect of TiB_2 volume content on the microstructure and mechanical properties of the composites was attentively investigated, and the strengthening and toughening mechanism was discussed.

2. Experimental procedure

2.1. Materials preparation

We selected commercially available powders of TiH_2 (99.9%, 300 mesh), Si (99.9%, 300 mesh), graphite (99.9%, 200 mesh), and B_4C (99%, average particle size 3.5 μm) as starting materials. The volume fraction of TiC in the composites was fixed at 10 vol.%, and that of TiB_2 was 5 vol.%, 10 vol.%, 15 vol.% and 20 vol.%, respectively. After being mixed and dried, the powder mixtures were compacted uniaxially under 10 MPa in graphite mold pre-sprayed with a layer of BN. The compacted mixture was first heated in an Ar atmosphere at a rate of 30 °C/min from room temperature to 900 °C and held for 1 h, and then heated to the sintering temperature of 1500 °C. The holding time was 2 h and the applied pressure was 25 MPa. Finally, the sample was furnace cooled down to room temperature.

2.2. Characterization

The density of (TiB_2 + TiC)/Ti_3SiC_2 composites was determined by the Archimedes method, and the phase identification of the materials was performed by X-ray diffractometer (ARL X'TRA, Switzerland) with Cu Kα radiation. The microstructures, fracture surfaces and crack propagation of the samples were investigated by scanning electron microscopy (SEM). Transmission electron microscope (TEM) was also used to observe the microstructure of the composites. The sintered materials were cut, ground and polished into strips with the size of 4 mm × 3 mm × 40 mm and three point bending was applied to measure room temperature bending strength using a span of 40 mm with a crossing speed of 0.5 mm/min. The fracture toughness (K_{IC}) was measured using single-edge notched beam (SENB) specimens with a size of 4 mm × 3 mm × 40 mm. The notch with a depth of 4 mm and width ≤0.28 mm was made. The crosshead speed for fracture toughness testing was 0.05 mm/min. Five samples were used in both strength and toughness measurements. Indentation tests were employed to determine Vickers hardness at room temperature using a Vickers' diamond indenter. The indention parameters were made using a load of 9.8 N with a dwell time of 10 s. Five measurement runs were carried out to determine the average value.

3. Results and discussion

3.1. Thermodynamic analysis

During the hot pressing sintering process, TiH_2 decomposes at about 900 °C and then the as-produced Ti reacts with other raw materials as follows:

$$TiH_2 \rightarrow Ti + H_2\uparrow \quad (1)$$

$$3Ti + Si + 2C \rightarrow Ti_3SiC_2 \quad (2)$$

$$Ti + C \rightarrow TiC \quad (3)$$

$$3Ti + B_4C \rightarrow 2TiB_2 + TiC \quad (4)$$

The thermodynamic calculation [16] indicated that the ΔG^{θ} of reaction (4) is $-634.4\ kJ\ mol^{-1}$ to $-622.4\ kJ\ mol^{-1}$ in the temperature range from 1350 °C to 1600 °C, in which reaction (2) can proceed sufficiently and Ti_3SiC_2 can exist stably [17]. This means that reaction (4) can take place forward in this temperature range. Therefore, in situ synthesis of (TiB_2 + TiC)/Ti_3SiC_2 composites with TiH_2, Si, graphite and B_4C powders as raw materials is thermodynamically feasible at the present sintering temperature. The general reaction in the present system can be described as follows:

$$(3+3x+y)TiH_2 + Si + (2+y)C + xB_4C \rightarrow Ti_3SiC_2 + 2xTiB_2 + (x+y)TiC + (3+3x+y)H_2\uparrow \quad (5)$$

The content of reinforcing agents TiB_2 and TiC can be adjusted by changing the value of x and y. In this work, excess Si (1.2 moles of Si) was added to insure the obtained TiC volume content in (TiB_2 + TiC)/Ti_3SiC_2 composites close to theoretical one. Using TiH_2 powder instead of Ti powder as Ti resource can produce an uncontaminated and high activity Ti powder, which will facilitate the in situ synthesis process and should be favorable to the optimization of microstructure and the improvement of properties.

3.2. X-ray diffraction characterization and sintering properties

Fig. 1 gives the X-ray diffraction patterns of (TiB_2 + TiC)/Ti_3SiC_2 composites with different volume content of TiB_2. All the samples show the same phase composition, i.e., Ti_3SiC_2 is the main phase, TiB_2 and TiC are the second phases. This suggests that in situ synthesis reactions described above have proceeded completely and in situ (TiB_2 + TiC)/Ti_3SiC_2 composite ceramics have been obtained. With the increase of the content of TiB_2, TiB_2 peaks increase with no obvious variation for Ti_3SiC_2 and TiC peaks. Fig. 2 shows that the samples prepared in this work are fully dense (apparent porosity is lower than 0.15%). Increase of TiB_2 content has no influence on the densification process of the composites. The weak variation in bulk density is due to the similar density among the three phases.

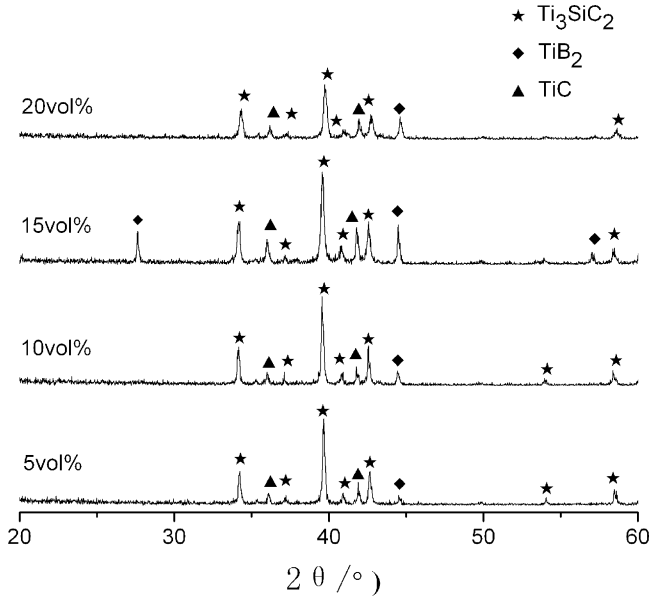

Fig. 1. XRD patterns of the materials with different TiB_2 content.

3.3. Microstructure

Fig. 3 shows TEM images and energy-dispersive X-ray spectroscopy (EDS) analysis results of the composite containing 10 vol.% TiB_2. The successful synthesis of (TiB_2 + TiC)/Ti_3SiC_2 composites was furthermore confirmed by EDS analysis. It can be seen that owing to the superiority of in situ synthesis, the grain boundaries are clean and clear. The reinforcing agent TiB_2 is small columnar grain with a length of about 1 μm and a slenderness ratio of 4. Fig. 4 shows the features of fractured surfaces of the composites with different TiB_2 content. Laminar Ti_3SiC_2 grains, columnar TiB_2 grains and equiaxed TiC grains were clearly identified. It can be seen from Fig. 4 that all the fractured surfaces are rough and there are pits and outcrops resulted from grain's pull out. The fracture mode consists of intergranular fracture mainly for Ti_3SiC_2 grains and transgranular fracture for TiB_2 and TiC grains. With the increment of TiB_2 volume content, the grain size of Ti_3SiC_2 matrix tends to decrease, which suggests that in situ addition of fine TiB_2 particles can evidently hinder the coarsening of Ti_3SiC_2 grains. In addition, with the increase of TiB_2 volume content, slenderness ratio of TiB_2 grains seems to decrease and agglomeration of TiB_2 particles is observed. It is known that TiB_2 is a brittle ceramic, which may make the cracks propagate through the composites easily. Therefore, the incorporation of excessive TiB_2 might adversely affect the bending strength and fracture toughness of the composites.

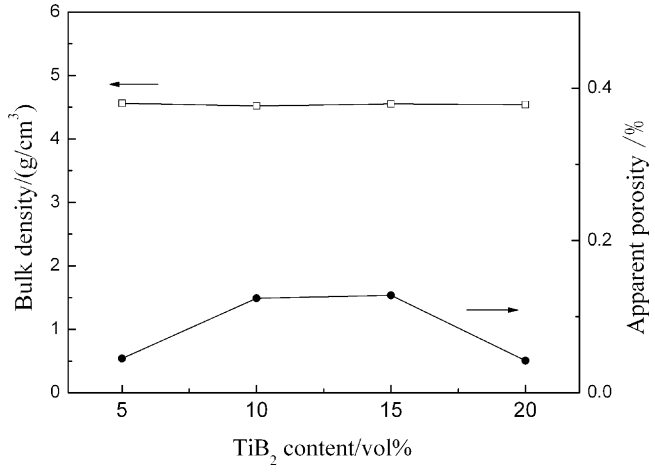

Fig. 2. Sintering properties of the materials with different TiB_2 content.

3.4. Mechanical properties

The bending strength and fracture toughness of (TiB_2 + TiC)/Ti_3SiC_2 composites are shown in Fig. 5. With the increase of TiB_2 content, the bending strength of the materials increases from about 500 MPa at 5 vol.% to 700 MPa at 10 vol.%, then decreases to about 400 MPa at 20 vol.%. A similar trend was found for the fracture toughness. Therefore, when TiB_2 content is about 10 vol.%, the optimal mechanical properties of 700 MPa for bending strength and 9.55 MPa $m^{1/2}$ for fracture toughness were obtained. These are much higher than the values of pure Ti_3SiC_2 ceramic and other Ti_3SiC_2-matrix composites [10,18], which suggests a significant strengthening and toughening effect.

The Vickers hardness of (TiB_2 + TiC)/Ti_3SiC_2 composites with the indentation load of 9.8 N is plotted in Fig. 6. It indicates that the hardness increases from 6.13 GPa to 11.5 GPa with TiB_2 volume content increasing from 5 vol.% to 20 vol.%. It can also be identified that the increase of Vickers hardness of the composites follows the linear relation

$$H_v\ (\mathrm{GPa}) = 4.085 + 0.3794V_f \quad (6)$$

Ti_3SiC_2 has a low hardness of about 4.3 GPa, but TiC and TiB_2 have a high hardness of about 27 GPa and 34 GPa, respectively. The incorporation of TiC and TiB_2 could effectively improve the Vickers hardness of the composites.

4. Discussion

As has been demonstrated in Fig. 4, the fractured surfaces of (TiB_2 + TiC)/Ti_3SiC_2 composites are rough and the fracture mode consists of intergranular fracture mainly for Ti_3SiC_2 grains and transgranular fracture for TiB_2 and TiC grains. In addition, pits and outcrops resulted from grain's pull out were observed.Owing to very close interatomic distance of close-packed plane of atoms for TiB_2 (0.3028 nm) and TiC (0.3055 nm), a coherent interface with strong binding energy will form between TiB_2 and TiC grains in the composites, which will result in transgranular fracture and increase fracture energy. The strengthening effect of TiB_2 results from its high hardness and high Young's modulus (550 GPa), which will lead to higher deformation resistance and residual stress toughening. When a composite is cooled down from the

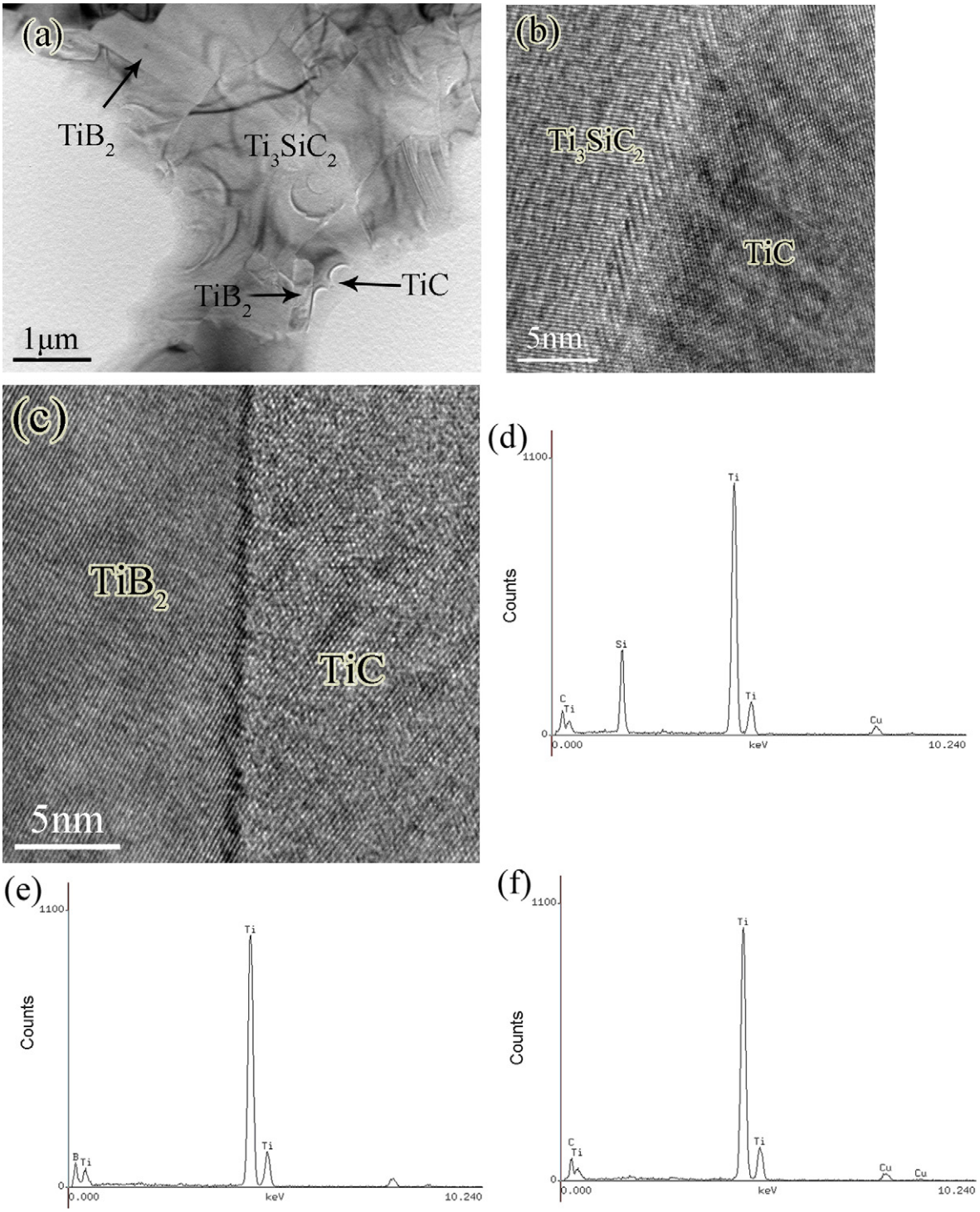

Fig. 3. (a) TEM images of the material with 10 vol.% TiB_2, (b) HRTEM image of interface structure for Ti_3SiC_2 and TiC, (c) HRTEM image of interface structure for TiB_2 and TiC, (d) energy-dispersive X-ray spectroscopy analysis of Ti_3SiC_2 grains, (e) energy-dispersive X-ray spectroscopy analysis of TiB_2 grains, and (f) energy-dispersive X-ray spectroscopy analysis of TiC grains.

fabrication temperature, thermal residual stress arises due to the thermo-elastic mismatch between constituents [19]. The CTEs of both TiB_2 and TiC are lower than that of Ti_3SiC_2 (the CTEs of Ti_3SiC_2, TiB_2 and TiC are 9.1×10^{-6}/K, 8.1×10^{-6}/K and 7.4×10^{-6}/K, respectively), therefore the residual stresses at the Ti_3SiC_2/TiB_2 and Ti_3SiC_2/TiC interfaces are in a compressive stress [20], which can make the cracks be deflected and propagate along the grain boundary as they meet the particles TiB_2 or TiC. Therefore, the crack path becomes zigzag and prolonged, consuming a lot of fracture energy. This is also advantageous to the strength and toughness of the composites.

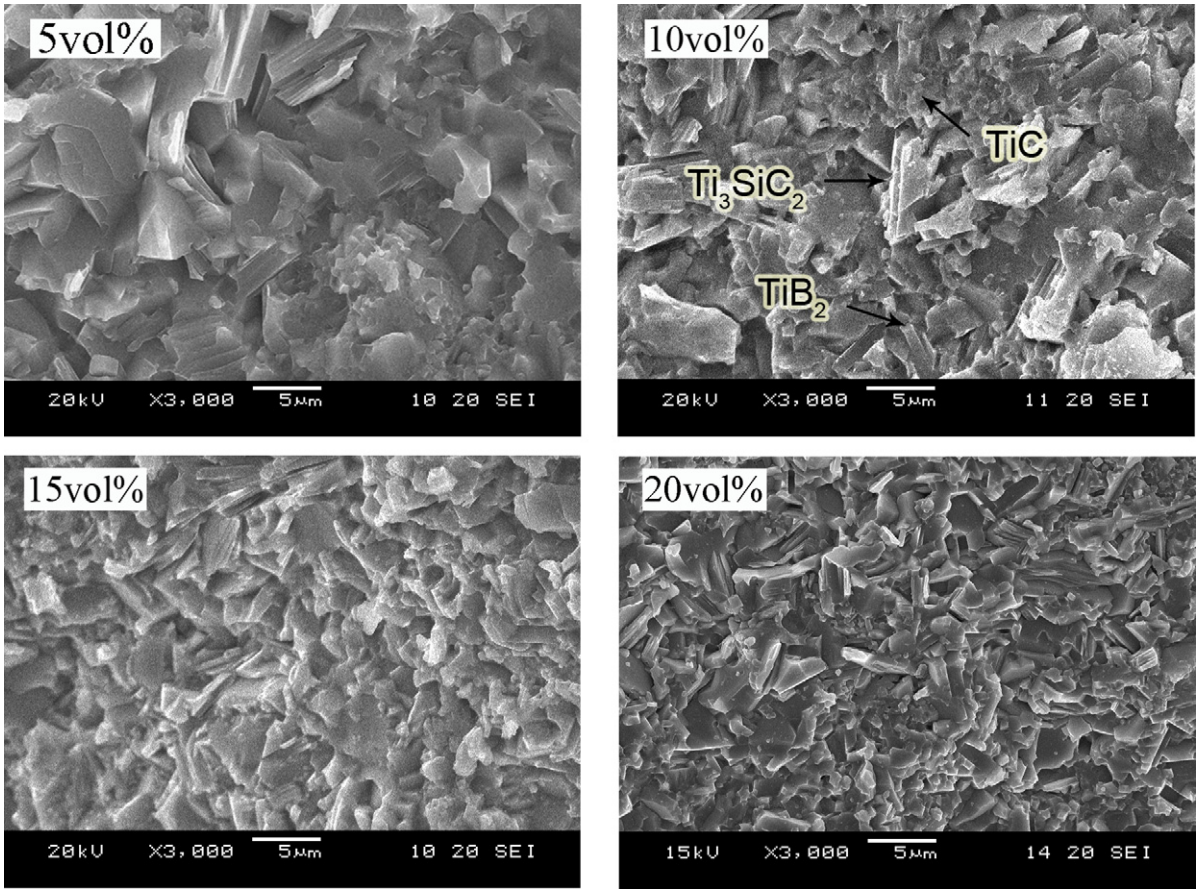

Fig. 4. SEM micrographs of fracture surfaces for the materials with different TiB_2 content.

Fig. 7 is the indentation morphology for the composite with 10 vol.% TiB_2 under the load of 9.8 N, which shows the typical characteristic of indentations for ternary layered carbides, i.e., localized damage occurs in the neighborhood of indentation and no crack propagation was found along the diagonal direction of indentation. This phenomenon also suggests a high resistance to damage and correspondingly high fracture toughness for (TiB_2 + TiC)/Ti_3SiC_2 composites.

As has mentioned above, the toughening mechanism of grain's pull out is also applicable for the composites which will also consume the energy applied by external environment through overcoming the friction coming from the neighborhood grains during the pulling out process. In addition, the incorporation of TiB_2 and TiC reinforcing agents significantly

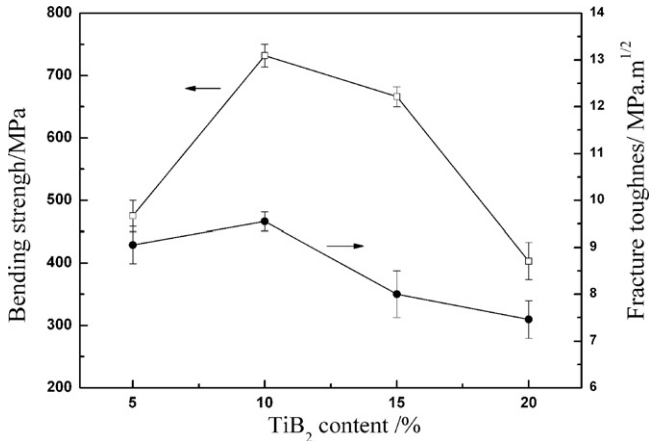

Fig. 5. Bending strength and fracture toughness of the materials (error bar: standard deviation).

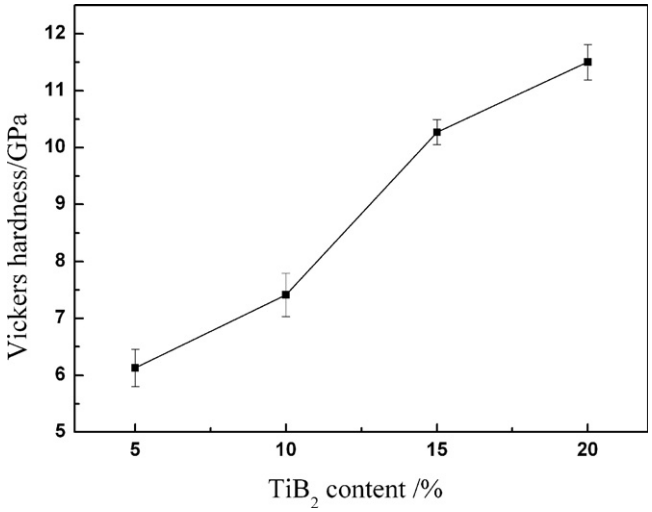

Fig. 6. Vickers hardness of the materials with different TiB_2 content (error bar: standard deviation).

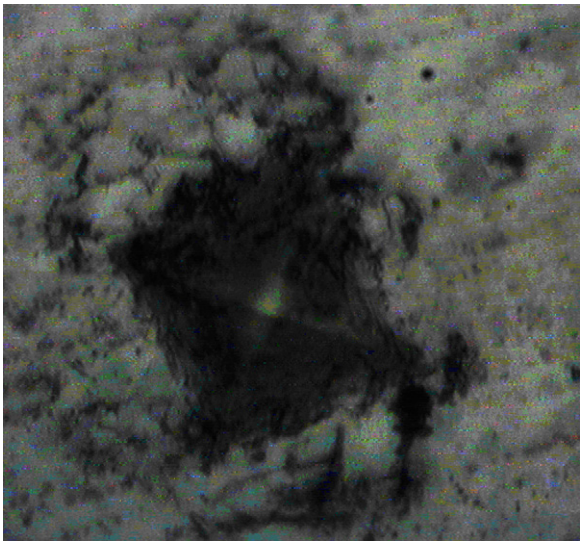

Fig. 7. SEM image of the indentation morphology for the material with 10 vol.% TiB_2 under the load of 9.8 N.

inhibits the grain-boundary migration of Ti_3SiC_2, resulting in a fine-grained Ti_3SiC_2 matrix. Hall–Petch equation [21] describes the relation between the yield stress point and the grain size.

$$\delta_y = \delta_0 + kd^{-1/2} \tag{7}$$

where δ_y is the yield stress for a polycrystal, δ_0 is the yield stress for a single crystal or a polycrystal with an infinitely large grain size, d is the average grain size, and k is the Hall–Petch parameter. Therefore, the increase of TiB_2 content will induce a grain refinement effect and improve the strength.

Fig. 8 shows magnified image of crack propagation path in the composite with 10 vol.% TiB_2 under the load of 490 N. The cracks show deflection, branching and bridging during propagation. This feature consumed the propagation energy and benefited for improving the fracture toughness. When TiB_2 content exceeds 10 vol.%, it is assumed that agglomeration of TiB_2 becomes serious in the composites, which eventually results in a decrease in the toughness.

In short, the composite with 10 vol.% TiB_2 shows the optimized fine microstructure, in which the synergistic action of the strengthening and toughening mechanisms such as particulate reinforcement, crack deflection, grain's pull-out and fine-grain toughening resulted in the excellent mechanical properties.

5. Conclusions

(1) Highly dense (TiB_2 + TiC)/Ti_3SiC_2 composite ceramics with different TiB_2 volume contents were in situ fabricated by hot-pressing at 1500 °C. Laminar Ti_3SiC_2 grains, columnar TiB_2 grains, equiaxed TiC grains and clean grain boundaries were clearly observed. Increase of TiB_2 volume content shows no influence on densification process of the composites, but significantly inhibits the grain growth of Ti_3SiC_2 matrix.

(2) When the content of TiB_2 increases from 5 vol.% to 20 vol.%, both bending strength and fracture toughness of the composites increase and then decrease. The maximum of 700 MPa for bending strength and 9.35 MPa $m^{1/2}$ for fracture toughness occurs at 10 vol.% TiB_2. The Vickers hardness increases linearly from 6 GPa to 11.5 GPa.

(3) The composite with 10 vol.% TiB_2 shows the optimized fine microstructure and optimal mechanical properties. These should be attributed to the synergistic action of the strengthening and toughening mechanisms such as particulate reinforcement, crack deflection, grain's pull-out and fine-grain toughening, which caused by the columnar TiB_2 grains and equiaxed TiC grains.

Acknowledgements

This work was supported by the National Natural Science Foundation of China under Grant No. 50872052, National High Technology Research and Development Program ('863' project) under Grant No. 2009AA05Z313, Natural Science

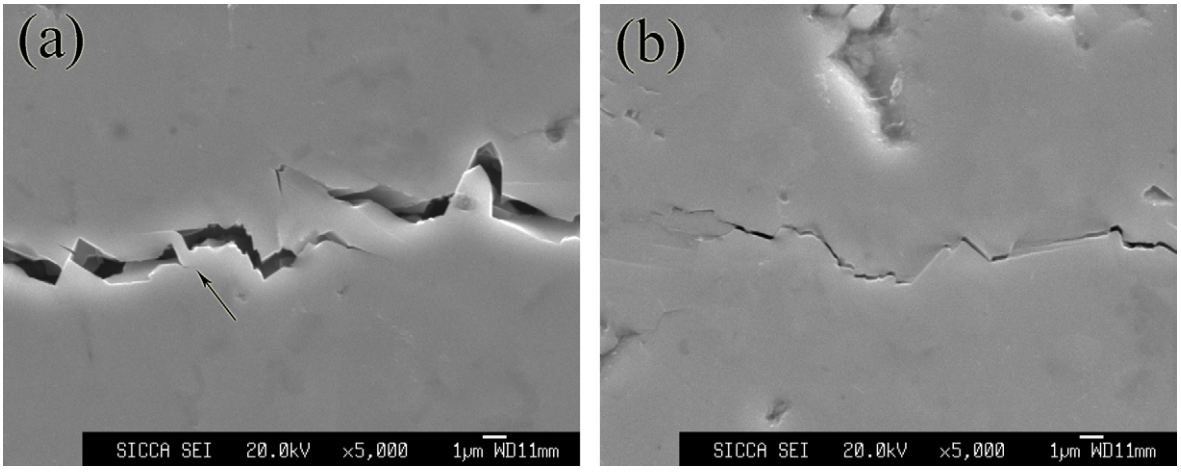

Fig. 8. Crack propagation path of the material with 10 vol.% TiB_2: (a) deflection and bifurcation of crack; (b) crack tip.

Foundation of Jiangsu Province Education Commission under Grant No. 07KJB430039, and the Key Laboratory of New Inorganic Materials and Its Composites, Jiangsu Province.

References

[1] M.W. Barsoum, The $M_{N+1}AX_N$ phases: a new class of solids; thermodynamically stable nanolaminates, Prog. Solid State Chem. 28 (1–4) (2000) 201–281.

[2] V.D. Jovic, B.M. Jovic, S. Gupta, et al., Corrosion behavior of select MAX phases in NaOH, HCl and H_2SO_4, Corros. Sci. 48 (12) (2006) 4274–4282.

[3] M. Radovic, M.W. Barsoum, A. Ganguly, et al., On the elastic properties and mechanical damping of Ti_3SiC_2, Ti_3GeC_2, $Ti_3Si_{0.5}Al_{0.5}C_2$ and Ti_2AlC in the 300–1573 K temperature range, Acta Mater. 54 (10) (2006) 2757–2767.

[4] H.I. Yoo, M.W. Barsoum, T. El-Raghy, Ti_3SiC_2 has negligible thermopower, Nature 407 (2000) 581–582.

[5] M.W. Barsoum, T. El-Raghy, Synthesis and characterization of a remarkable ceramic: Ti_3SiC_2, J. Am. Ceram. Soc. 79 (7) (1996) 1953–1956.

[6] C.F. Hu, Y.C. Zhou, Y.W. Bao, et al., Tribological properties of polycrystalline Ti_3SiC_2 and Al_2O_3-reinforced Ti_3SiC_2 composites, J. Am. Ceram. Soc. 89 (11) (2006) 3456–3461.

[7] J.F. Zhang, L.J. Wang, W. Jiang, et al., Effect of TiC content on the microstructure and properties of Ti_3SiC_2–TiC composites in situ fabricated by spark plasma sintering, Mater. Sci. Eng. A 487 (1–2) (2008) 137–143.

[8] J.F. Zhang, L.J. Wang, W. Jiang, et al., Rapid fabrication of Ti_3SiC_2–SiC nanocomposite using the spark plasma sintering-reactive synthesis (SPS-RS) method, Scripta Mater. 56 (3) (2007) 241–244.

[9] E. Benko, P. Klimczyk, S. Mackiewicz, et al., cBN–Ti_3SiC_2 composites, Diamond Relat. Mater. 13 (3) (2004) 521–525.

[10] W.B. Zhou, B.C. Mei, J.Q. Zhu, Synthesis of Ti_3SiC_2/TiB_2 composite by in-situ hot pressing (HP) method, J. Wuhan Univ. Technol. – Mater. Sci. Ed. 23 (6) (2008) 863–865.

[11] S.L. Shi, W. Pan, Toughening of Ti_3SiC_2 with 3Y-TZP addition by spark plasma sintering, Mater. Sci. Eng. A 447 (1–2) (2007) 303–306.

[12] J.X. Chen, J.L. Li, Y.C. Zhou, In-situ synthesis of Ti_3AlC_2/TiC–Al_2O_3 composite from TiO_2–Al–C system, J. Mater. Sci. Technol. 22 (4) (2006) 455–458.

[13] Q.F. Zan, L.M. Dong, C. Wang, et al., Improvement of mechanical properties of Al_2O_3/Ti_3SiC_2 multilayer ceramics by adding SiC whiskers into Al_2O_3 layers, Ceram. Int. 33 (3) (2007) 385–388.

[14] K.S. Cho, H.J. Choi, J.G. Lee, et al., In situ enhancement of toughness of SiC–TiB_2 composites, J. Mater. Sci. 33 (1998) 211–214.

[15] G.J. Zhang, Z.Z. Jin, In-situ synthesis of ceramic composites, Mater. Rev. 10 (2) (1996) 62–65.

[16] Y.J. Liang, Y.C. Che, Handbook of Thermodynamic Properties for the Inorganic Substances, Northeastern University Press, Shenyang, 1993.

[17] R. Radhakrishnan, J.J. Williams, M. Akinc, Synthesis and high-temperature stability of Ti_3SiC_2, J. Alloys Compd. 285 (1) (1999) 85–88.

[18] S. Konoplyuk, T. Abe, T. Uchimoto, et al., Synthesis of Ti_3SiC_2/TiC composites from TiH_2/SiC/TiC powders, Mater. Lett. 59 (18) (2005) 2342–2346.

[19] J.F. Bartolomé, G. Bruno, A.H. DeAza, Neutron diffraction residual stress analysis of zirconia toughened alumina (ZTA) composites, J. Eur. Ceram. Soc. 28 (9) (2008) 1809–1814.

[20] J. Selsing, Internal stresses in ceramics, J. Am. Ceram. Soc. 44 (8) (1961) 419–426.

[21] R.W. Rice, C.C. Wu, F. Borchelt, Hardness–grain-size relations in ceramics, J. Am. Ceram. Soc. 77 (10) (1994) 2539–2553.